Journal of Materials Chemistry A

Accepted Manuscript

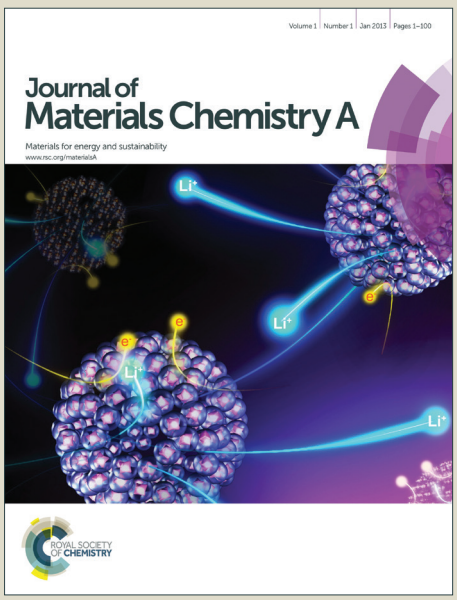

ROYAL SOCIETY OF CHEMISTRY

www.rsc.org/materialsA

Journal of Materials Chemistry A RSCPublishing

ARTICLE

Cite this: DOI: 10.1039/x0xx00000x

Ultrafast Charge Transfer in Solid-State Films of Pristine Cyanine Borate and Blends with Fullerene

Jelissa De Jonghe-Risse,[a] Jakob Heier,[b] Frank Nüesch,[b,c] and Jacques-E. Moser[a] *

Received 28th November 2014,
Accepted 00th April 2015

DOI: 10.1039/x0xx00000x

www.rsc.org/

Photoinduced electron transfer in light-absorbing materials is the first step towards charge separation and extraction in small molecule-based organic solar cells. The excited state dynamics of the cyanine dye cation Cy3 paired with a tetraphenylborate counter-anion (Cy3-B) was studied in pristine solid-state films of the dye and in blends with the electron acceptor material PCBM. Here we show that photoexcited Cy3-B in pure films undergo intra-ion pair reductive quenching on the picosecond time scale, while in blends with PCBM sub-picosecond formation of the Cy3 oxidized species is observed upon electron injection from the dye excited state into the fullerene. Kinetic competition between light-induced electron- and hole transfer processes strongly depends on the PCBM content in the blends. A high PCBM loading produces a fully intermixed phase, where the cyanine oxidized states appear on ultrashort (<160 fs) time scales. Lower PCBM contents, on the contrary, lead to a Cy3-B segregated phase on top of the intermixed phase and slower excited state quenching. These findings show that the phase morphology indeed controls in a large extent the efficiency of primary photoinduced charge separation, on which small molecule-based organic photovoltaic cells are relying.

Introduction

Continuous progresses in small molecule organic solar cells technology has lead lately to promising power conversion efficiencies.[1-3] Efforts are currently pursued towards improved stability and device performances. The increasing interest for these systems and the need for a better knowledge of the initial charge generation have lead researchers to thoroughly investigate primary ultrafast photoinduced processes.[4,5] Solar cells built from cyanine dyes and fullerene electron acceptor are particularly interesting. Indeed, spontaneous phase de-mixing in blends of the two materials forms bulk heterojunctions characterized by a rich variety of phase morphologies.[6] On the other hand, bilayer solar cells based on the cyanine dye Cy3 (1,1'-diethyl-3,3,3',3'-tetramethylcarbocyanine, see structure in Figure 1), in particular, have shown competitive photovoltaic power conversion efficiency, reaching up to 3.7%.[7-12] Cyanines are positively charged polymethine dyes and are paired with a negatively charged counter-ion. Anion migration under applied electric fields in solid state cyanine layers has been observed and could be detrimental for small molecule solar cell applications, as the charges building up at the electrode interface would hinder charge extraction.[6,13] In order to restrict ion migration, larger counter-anions can be used such as borate and trisphat.[14] Their redox photoactivity has nonetheless to be controlled in order to avoid irreversible reactions. The photophysical properties of cyanine dyes have been extensively studied in solution,[15-17] and in pristine solid-state films.[18-20] Cy3 excited state dynamics in solution are strongly dependent on the nature of the counter-anion.[21-25] Cy3 hexafluorophosphate (Cy3-P) tends to photoisomerize to the *cis*-isomer and has a rather poor fluorescence quantum yield. The excited state decays in a few hundreds of picoseconds, while the *cis*-isomer absorbing at 580 nm is characterized by a microsecond lifetime. With the iodide counter-anion, no singlet excited state is observed on the ps time scale, but rather a triplet excited state with nanosecond lifetime absorbing at 620 nm is formed due to the heavy-atom effect of iodine, enhancing intersystem crossing. In the case of borate counter-anions, it has been shown that electron transfer to the excited state of the cyanine (reductive quenching) leads to a reduced dye species ($Cy3^{-}$), which absorption is centered at a wavelength of 430 nm. Alkyl-substituted borates undergo a carbon-boron bond cleavage upon oxidation, generally resulting in unstable product radicals. However, in the case of tetraphenylborate, which is a good electron donor,[26,27] back-electron transfer from the reduced cyanine species is apparently sufficiently fast to regenerate the dye borate and prevent its decomposition.

The photophysical processes for the cyanine tetraphenylborate salt that undergoes intra ion-pair electron transfer under light irradiation are shown in Figure 1 (process 2). By adding an electron acceptor such as the fullerene derivative [6,6]- phenyl C_{61}-butyric acid methyl ester (PCBM), kinetic competition between electron transfer to PCBM (process 1) and reductive quenching by tetraphenylborate (process 2) is expected.

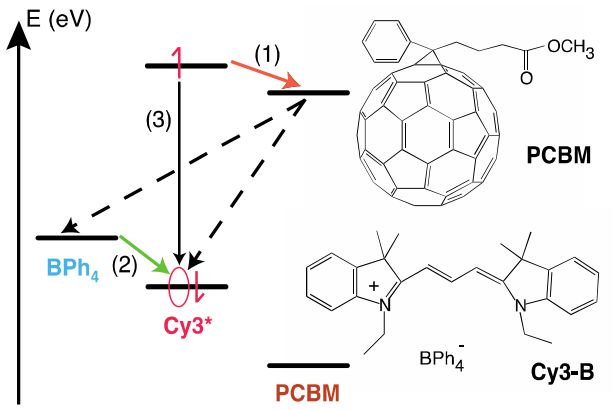

Figure 1. Schematic layout of energy levels and electron transfer processes following Cy3 photoexcitation in pristine Cy3-B and blends with PCBM. (1) Electron transfer from Cy3 LUMO to PCBM; (2) reductive quenching of Cy3* excited state by the tetraphenylborate counter-anion (e^- transfer from BPh_4 to Cy3 HOMO); (3) deactivation of Cy3* through radiative and non-radiative pathways. Back-electron transfer and charge recombination at tetraphenylborate|PCBM junctions appear as dotted lines. The molecular structures of the investigated materials are shown on the right.

$$Cy3^* + PCBM \rightarrow Cy3^+ + PCBM^- \quad (1)$$

$$Cy3^* + BPh_4 \rightarrow Cy3^- + BPh4^+ \quad (2)$$

In this work we report transient absorption studies on solid-state films of pristine cyanine tetraphenylborate (Cy3-B) and of various blends with PCBM. Kinetic competition between the reductive quenching by tetraphenylborate of the photoexcited Cy3 (Eq. 2) and its oxidative quenching by PCBM (Eq. 1) was monitored. Different PCBM:Cy3-B blend ratios enabled to alter the yield of the oxidized cyanine ($Cy3^+$), indicating that intermixed phases are crucial for photoinduced charge separation.

Results and discussion

Femtosecond pump-probe experiments were carried out on the various film compositions. As the photoabsorption of different species overlap in the visible spectral range, a series of blends was investigated, whose composition was varied from pure Cy3-B up to a molar ratio PCBM:Cy3-B of 15.5:1. The normalized absorption spectra of thin films of pristine Cy3-B and of bulk heterojunctions formed in blends with PCBM are shown in Figure 2. Pristine Cy3-B ground state absorption spectrum in solid films extends over wavelengths from approximately 450 to 600 nm and displays the dye's monomer absorption maximum at 570 nm. This spectrum is similar to that of the Cy3-P cyanine dye with PF_6^- as a counter-anion.[8] It is red-shifted and broadened compared to the absorption spectrum measured in solution. Blue shifted features are attributed to dimers and H-aggregates absorption (shoulder around 500 nm). Remarkably, the amount of aggregated dye is rather small and does not seem to increase in the presence of PCBM. Absorption of PCBM is quite weak in the visible but increases in the UV region, causing a slight blue shift of the apparent Cy3-B absorption maximum in blends.

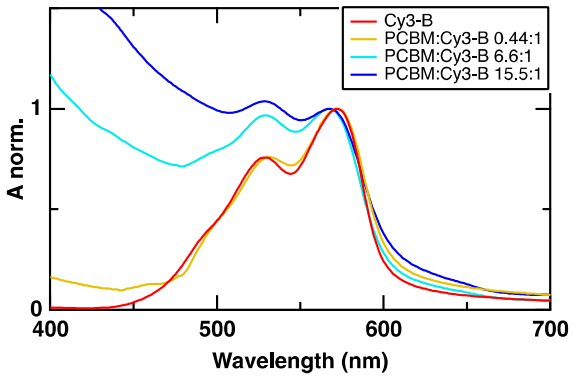

Figure 2. Normalized steady-state absorption spectra of the pristine Cy3-B film and the various blends with PCBM.

Pristine Cy3-B

For clarity of the discussion, transient absorption results for pristine Cy3-B are presented first. Upon pulsed laser excitation, appearance of a large negative band located at 550-680 nm is observed instantaneously (Figure 3a) and is attributed to the Cy3 ground-state bleaching (GSB) due to the similarity with steady-state absorbance (Figure 2). At early time delays, the negative maximum at 580 nm contains contributions of both the GSB and of a weak stimulated emission signal (SE). As the SE vanishes, this maximum shifts to the blue to 570 nm. The positive transient absorption band observed at 420-500 nm during the first tenths of picoseconds is assigned to the singlet excited state absorption (ESA), which was already reported by Chatterjee et al. for time-resolved flash photolysis studies on Cy3-P.[24,28] This photoabsorption compensates the GSB below 550 nm. The fast quenching of the cyanine ESA by the

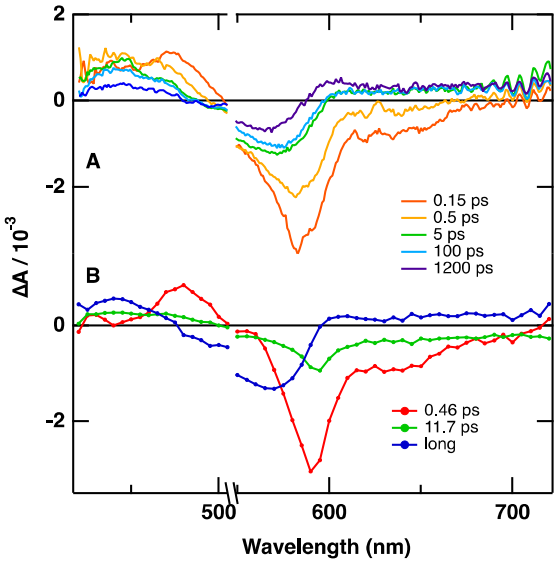

Figure 3. a) Transient absorption spectra at various time delays after 530 nm excitation for pristine Cy3-B and b) Amplitude spectra associated to the time constants resulting from the multiexponential global analysis for pristine Cy3-B.

tetraphenylborate counter-anion leads to the formation of the reduced cyanine species ($Cy3^{-}$) absorbing at about 420-470 nm and oxidized tetraphenylborate (Eq. 2). This reductive quenching reaction has been observed in solution.[25] In thin solid films, red shift and broadening of the absorption spectra compared to the same species in solution is commonly observed for molecules, which explains a maximum absorption peak for the $Cy3^{-}$ species located at 420-470 nm in the pristine film compared to 430 nm in solution.

Kinetic data were recorded with pulsed laser excitation energy fluence at the sample of 45 μJ/cm^2. No effect of the light intensity was observed, as evidenced by identical dynamics obtained upon application of lower fluences (Figure S1 a). The associated spectra resulting from a multiexponential global analysis are shown in Figure 3 b. They bring clear evidence for the reductive quenching mechanism. More details about the procedure applied for the global analysis of multiwavelength kinetic data are provided in electronic supplementary information. The decay of the red part of the ESA between 460-500 nm is associated with a 0.46 ps time constant and is mirrored by the decay of the SE around 590-680 nm. As the GSB does not decay on this time scale, it is reasonable to assume that the singlet excited state does not fully return to the ground state, and this will be confirmed later. Looking more specifically at the positive transient feature located at 420-460 nm and assigned to both the ESA and $Cy3^{-}$ absorption, it is clear that the ESA is converted into the reduced cyanine species transient signal with a time constant of 0.46 ps. The reductive quenching of the excited state by the tetraphenylborate counter-anion is evidenced by the isosbestic point located at 460 nm (Figure 3b) between the red part of the ESA and the absorption of the reduced cyanine. The latter signal grows with an 11.7 ps time constant and displays a lifetime that is longer than the 1 ns maximum optical time delay available with our femtosecond laser setup. Application of nanosecond flash photolysis measurements to identical samples (Fig. 4) confirmed the formation of long-lived reduced cyanine species, whose decay by back electron transfer takes place in the microsecond time scale. Complete regeneration of the dye was achieved within 200 μs, which is then compatible with the 1 kHz repetition rate of ultrafast transient absorption experiments.

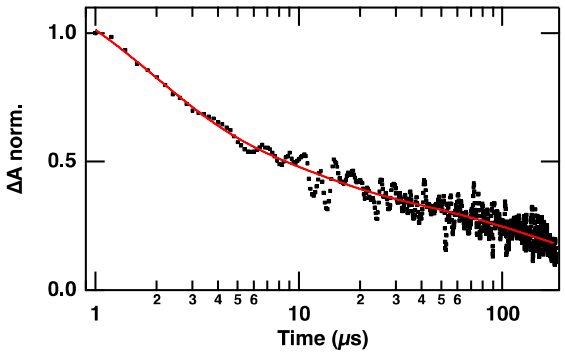

Figure 4. Dynamics recorded at 450 nm probe after 530 nm excitation for pristine Cy3-B. The solid line is the best fit of experimental data points.

Blends with PCBM

The morphology of bulk heterojunctions in blended PCBM|Cy3-B films depends on the relative amount of the fullerene acceptor material. This behaviour is qualitatively similar to that of previously described PCBM|Cy7-trisphat blend films.[29] Films prepared with the largest PCBM loading (15.5:1) display only one fully intermixed phase, while lower PCBM amounts lead to both intermixed and pure cyanine phases segregating at the surface. In the latter case, phase contrast AFM images reveal a spinodal phase pattern at the surface (Fig. S2 a). Dipping samples into tetrafluoropropanol solvent selectively dissolves the pure dye phase. Remaining films contain intermixed Cy3-B with PCBM, none of the materials being dissolved anymore. The topography reflects the inverse structure of the dye surface domains (Fig. S2 b). The various morphologies obtained for different compositions can be explained with an asymmetry in the PCBM|dye|solvent ternary phase diagram and the nature of film formation during a solvent quench (Fig. S3).[29] At high PCBM loadings, the system remains in the one phase region (fully intermixed) for all solvent concentrations. For lower PCBM loadings, solvent evaporation brings the system into a two-phase region. It is however unclear how molecular intercalation of PCBM in the cyanine tetraphenylborate ion-pair occurs in the intermixed phase.

The lower the PCBM loading, the largest the pure cyanine layer. The intermixed phase leads to a direct competition between electron transfer to PCBM (Eq. 1) and reductive quenching by the tetraphenylborate counter-anion (Eq. 2) following light absorption by Cy3. As a pure Cy3-B phase exists in all sample, except in the 15.5:1 blend, a transient absorption signal corresponding to the $Cy3^{-}$ species obtained by reductive quenching is expected. Direct light absorption by PCBM can be neglected for the low content sample (0.44:1), while blends with higher fullerene molar ratio show about 20% light absorption by the sole PCBM material (Figure 2). The ground-, excited-, and reduced states of PCBM have rather low extinction coefficients and are, therefore, not responsible for the majority of the transient absorption signals observed in the probed spectral range.[25] Oxidation of Cy3 upon hole transfer from photoexcited PCBM molecules, however, cannot be excluded.

The effect of the addition of PCBM on the dynamics observed at a probe wavelength of 440 nm, where both the Cy3 excited state and reduced species absorb, is shown in Figure 5 a. For all blends, the initial amplitude of the photoabsorption is reduced compared to that of the pristine Cy3-B. This suggests that ultrafast quenching of the Cy3* excited state by PCBM is taking place, successfully competing with the reductive quenching by tetraphenylborate and inhibiting the formation of $Cy3^{-}$. The dynamics recorded at 550 nm shown in Figure 5 b are assigned to both the GSB of the cyanine and to the absorption of $Cy3^{+}$ species formed in blends.[7] At this wavelength a local minimum is observed in the dye ground state absorption spectrum (see Fig. 2), which enables

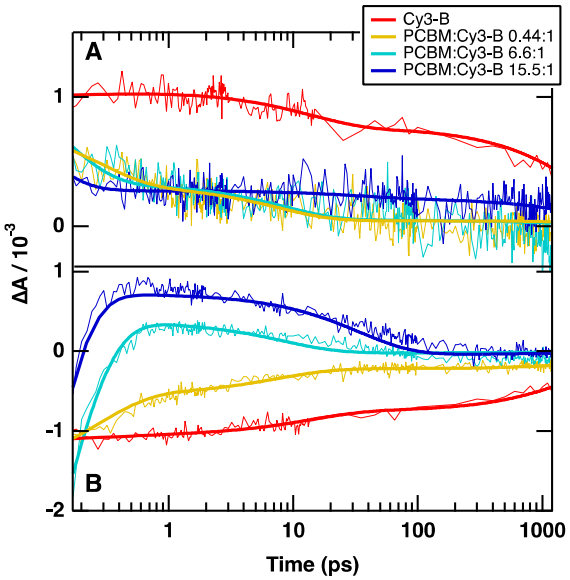

Figure 5. Dynamics recorded after 530 nm excitation for pristine Cy3-B and various PCBM loadings for a) 440 nm (Cy3 excited and reduced state) and b) 550 nm (Cy3 GSB and oxidized state) probe wavelengths. The solid lines represent the result of the best multiexponential fit.

scrutinizing the formation of the oxidized cyanine species. At high PCBM loadings, photoabsorption of $Cy3^+$ is directly observed. The amplitude of the positive signal gradually increases with the PCBM content, indicating production of a higher amount of the oxidized cyanine. The dynamics of cyanine oxidized state formation is extremely fast and could not be entirely resolved with our ultrafast setup. The time constant for $Cy3^+$ formation yielded by the fitting procedure is, therefore, certainly overestimated. The amplitude values for the high PCBM content blends (6.6:1 and 15.5:1) can hardly be compared quantitatively as absorption by PCBM cannot be excluded. This explains the similar amplitudes measured at a wavelength of 440 nm for the 0.44:1 and 6.6:1 blends (Fig. 5 a). Signal amplitudes can be compared only for pristine Cy3-B and the 0.44:1 blend.

The fits shown in Figure 5 result from a global analysis of multiwavelength kinetic data. Figure 6 presents the associated amplitude spectra (amplitudes associated to the three time constants) for the photophysical processes observed in pristine Cy3-B and blends with PCBM as depicted in Figure 1. The transient absorption spectra for the blends are shown in Figure S4, and again a fluence of 45 μJ/cm^2 was chosen as no intensity effect was observed (Fig. S1) and a satisfying signal-to-noise ratio was obtained. The first two associated time constants for the blends are shown in Table 1, the longer being outside of the time window allowed by our femtosecond setup (> 1 ns). The shortest time constant (Fig. 6 a and Table 1) is associated to the Cy3 excited state quenching and the concomitant growth of either the oxidized or the reduced cyanine species absorptions upon electron transfer (Eq. 1) or reductive quenching (Eq. 2), respectively. A large negative amplitude located between 500-600 nm is observed for all

Film composition	Cy3* quenching time constants	$Cy3^-$ and $Cy3^+$ lifetime
Pristine Cy3-B	462.1 ± 17.7 fs (52 %) 11.7 ± 1.4 ps (48%)	$Cy3^-$: 10^{-4} s
PCBM:Cy3-B 0.44:1	261.1 ± 4.4 fs	$Cy3^+$: 10^{-10} s
PCBM:Cy3-B 6.6:1	132.0 ± 1.7 fs	$Cy3^+$: 10^{-10} s
PCBM:Cy3-B 15.5:1	77.5 ± 2.1 fs	$Cy3^+$: 10^{-10} s

Table 1. Time constants for Cy3* excited state quenching and approximate lifetimes (order of magnitude) of oxidized and reduced forms of the dye in films of various compositions.

blends (Fig. 6 a), which increases with increasing PCBM relative content and is directly related to the ultrafast formation of the oxidized cyanine species. When PCBM is added, the SE gradually disappears (Figure S4), but Cy3 ESA spanning over a wide range of wavelengths (420-500 nm) is still observed at early time delays. This indicates that ultrafast electron transfer to PCBM occurs from the cyanine emissive photoexcited state. For pure Cy3-B in either pristine Cy3-B dye films or in the segregated phase from blends, $Cy3^-$ absorption around 420-470 nm, starts growing on a similar time scale. As a result, no decaying amplitude associated to the first time scale is observed at the blue side of the ESA. The intermediate time scale, shown in Figure 6 b, reveals the presence of reduced dye species for all samples, except the one containing the highest PCBM load (15.5:1). This is an expected result, as this is the only sample where both Cy3-B and PCBM are fully intermixed, thus resulting in a fast electron transfer to the fullerene competing successfully against the reductive quenching by BPh_4. The oxidized state's lifetime is associated to the intermediate time constant (Fig. 6 b, picoseconds), whereas the reduced species lives for several microseconds (Figs 4, 6c and Table 1).

In solution, reductive quenching of C_{60} triplet photoexcited state by a tetraphenylborate anion has been observed to yield the C_{60} anion.[26] The PCBM anion absorbs around 1030 nm, outside of the spectral range covered by our setup.[30] Moreover, intersystem crossing to the triplet state of PCBM is rather improbable in thin films, as other deactivation pathways become possible due to the close packing of fullerene molecules.[31]

The positive amplitude of the absorption change observed at longer wavelengths for 15.5:1 and 6.6:1 blends (Figs 6 and S4) could be due to PCBM ESA, although fullerene molecules absorb only 20% of the incoming light. We are currently investigating the origin of this effect. Among various hypotheses, we could speculate that this photoabsorption originates from charge transfer states formed between cyanine and PCBM neighboring molecules.[32] Photoinduced Stark effect is excluded here, as the Stark shift observed elsewhere for Cy3-P is quite weak, and the one arising from PCBM typically displays narrow features, which do not appear here.[5,33]

While the yield of electron transfer from Cy3* to the fullerene clearly increases with the acceptor's concentration (Fig. 5b), its rate also appears to depend upon the PCBM molar ratio. Time constants measured for the cyanine excited state quenching are reported in Table 1. From results obtained with the pure Cy3-B

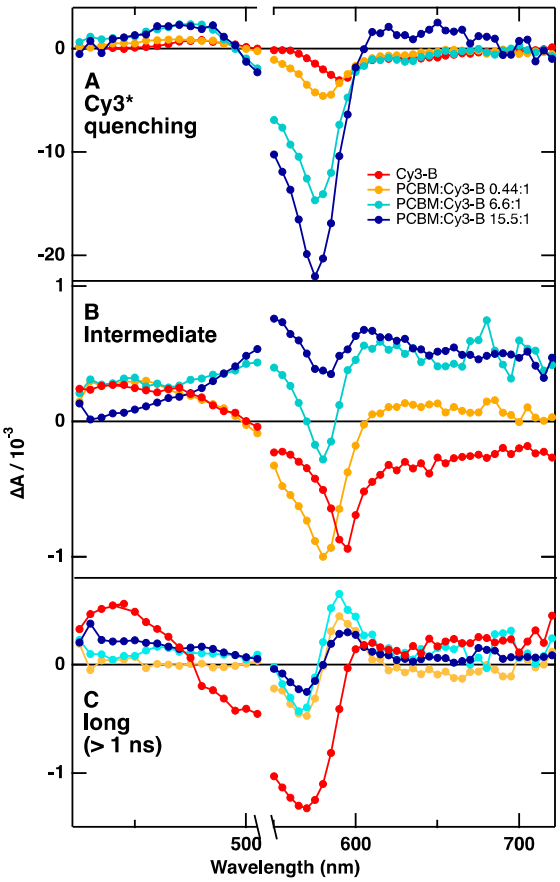

Figure 6. Associated amplitude spectra resulting from the multiexponential global analysis for the various investigated samples. a) is the excited state quenching, b) is the intermediate time scale (order of 100 ps) and c) is the long time scale (> 1ns).

sample, we can conclude that the reductive quenching happens in a few picoseconds (0.46 and 11.7 ps time constants). In the intermixed phase of blends, $Cy3^+$ species appear on time scales decreasing with the average distance separating Cy3 and PCBM molecules, reaching 77.5 fs for the 15.5:1 blend. As explained earlier in the text, the fit obtained for this sample probably overestimates the time constant (Fig. 5 b), whose actual value must probably be shorter than 50 fs. The cyanine oxidized state lifetime does not exceed a few tenths of picoseconds as evidenced in Figure 5 b. Figure 6 c showing the long time component corroborates this as no transient signal assigned to $Cy3^+$ around 550 nm is observed. Hole transfer from photoexcited PCBM in the 6.6:1 and 15.5:1 blends is not ruled out, and could also be responsible of a faster appearance of Cy3 oxidized state. The 0.44:1 blend still shows a faster excited state quenching than in pristine Cy3-B, whereas in this sample the absorption by PCBM is negligible. It is therefore clear that electron transfer from photoexcited Cy3 to PCBM is faster than the reductive quenching by tetraphenylborate, and that hole injection from photoexcited PCBM to Cy3 could be even faster. It is likely that reduction $Cy3^+$ species obtained upon electron transfer to PCBM by tetraphenylborate counter-anion is also responsible for the decay of the Cy3 oxidized species absorption. We expect that applying a voltage to the blend solar cell devices will prevent the unwanted charge recombination from the PCBM anion. The effect of a voltage bias will be treated in a separate paper.[33]

Cy3 isomerization is assumed to be responsible for the positive transient absorption feature observed at 600 nm on long time scales in blends only (Figure 6c). It is not observed in pristine Cy3-B, which leads to think that the isomerization, which is a rather slow process (ns), occurs in the intermixed phase. Either the ion pair with tetraphenylborate is too closely packed, resulting in inevitable reductive quenching upon light absorption by Cy3 in pure Cy3-B layers, or isomerization occurs from the cyanine oxidized species. Further investigations on the isomerization of cyanine dyes will be addressed in a future study.

Conclusions

In summary, we have shown that cyanine tetraphenylborate Cy3-B undergoes intra-ion pair reductive quenching in the solid state. The picosecond time scale for electron transfer from the tetraphenylborate moiety to the excited Cy3 suggested from the global analysis is in accordance with previous findings in solution.[19,20] No evidence for tetraphenylborate radical due to carbon-boron bond cleavage has been noticed as the cyanine reduced species absorbing at 420-450 nm recombines with the oxidized tetraphenylborate on the microsecond time scale. The widely used PCBM electron acceptor was blended with Cy3-B with different ratios and we found that the phase morphology drives charge injection in PCBM. High PCBM loadings consist of a fully intermixed phase, where $Cy3^+$ oxidized states appearance takes place readily after the excitation laser pulse (time constant < 160 fs). Low PCBM loadings lead to an intermixed phase and a pure Cy3-B segregated phase, therefore enabling the observation of both reduced and oxidized Cy3 species. The $Cy3^+$ oxidized species produced in the intermixed phase recombines on the hundred-picosecond timescale. Overall, observation of the cyanine species in either the oxidized or reduced form, resulting from kinetic competition between electron transfer to PCBM or intra ion-pair reductive quenching, is a sensitive indicator of the degree of intermixing of different phases. The better understanding of the dynamics of charge transfer in bulk heterojunctions provides ways to establish clear structure-property relations that will enable precise control of the optoelectronic properties in OPV materials by targeting optimized morphologies.

Experimental Part

Materials

The cyanine dye 1,1'-diethyl-3,3,3',3'-tetramethylcarbocyanine tetraphenylborate (Cy3-B) was purchased from FEW chemicals, Germany. [6,6]- phenyl C_{61}-butyric acid methyl ester (PCBM) was purchased from Solenne B.V., Netherlands. Both Cy3-B and PCBM were dissolved with various mole percent concentrations in chlorobenzene (Sigma-Aldrich). The

films were fabricated by spin coating the mixed solutions onto glass substrates. All the samples were prepared under nitrogen in a glove box. All chemicals were used as supplied, without further purification.

Spectroscopy

Absorption spectra were recorded on a Perkin-Elmer Lambda 950 spectrophotometer. Spectra were baseline-corrected and measured against a reference.

Transient absorption spectra were recorded with a femtosecond pump-probe spectrometer based on an amplified Ti-sapphire laser (Clark-MXR, CPA-2001) delivering 778 nm pulses of 150 fs duration at a 1kHz repetition rate. The pump beam was generated by a two-stage non-collinear optical parametric amplifier (NOPA), while the probe beam was a broadband white light continuum (420-720 nm) generated by a portion of the 778 nm fundamental output of the laser passing through a sapphire plate. The pump wavelength was set at 530 nm and the fluence at the sample was limited to 45 $\mu J/cm^2$. The probe beam was split before the sample into signal and reference beams in order to account for intensity fluctuations. Both beams were recorded shot by shot with a pair of 163 mm spectrographs (Andor Technology, SR163) equipped with 512 x 58 pixels back-thinned CCD cameras (Hamamatsu S07030-0906). The transient spectra were recorded by averaging over 3000 shots. The polarization of pump and probe pulses were set at magic angle. All time-dependent spectra were corrected for white-light chirp measured by Kerr gating and background noise. Global analysis by a multiexponential fit at different wavelengths (typically every 5 nm) allowed for unraveling the various occurring photophysical processes. The associated spectra show the amplitude of the transient signal related to each time component. The global analysis procedure is detailed in electronic supplementary information. The samples were analyzed in a dry argon atmosphere in a home-built chamber avoiding contact with ambient air.

Microsecond timescale dynamics were recorded using a frequency-tripled Q-switched Nd:YAG laser (Ekspla NT-342) running at 20 Hz repetition rate. An optical parametric oscillator was used to generate 530 nm wavelength pump pulses (5 ns FWHM). The continuous-wave probe light from a xenon lamp was transmitted through the sample, various optics, and a grating monochromator before being detected by a fast photomultiplier tube. Transient signals were recorded by a digital oscilloscope (Tektronix DPO 7104C). Averaging over typically 3000 shots yielded a satisfactory signal-to-noise ratio. A second-order Savitsky-Golay smoothing algorithm was applied (35 points intervals).

Acknowledgements

Financial support by NCCR-MUST and the Swiss National Science Foundation is gratefully acknowledged.

Notes and references

[a] Photochemical Dynamics Group, Institute of Chemical Sciences and Engineering, École Polytechnique Fédérale de Lausanne, CH-1015 Lausanne, Switzerland.
E-mail: je.moser@epfl.ch

[b] Laboratory for Functional Polymers, Swiss Federal Laboratories for Materials Science and Technology, EMPA, CH-8600 Dübendorf, Switzerland.

[c] Institute of Materials, École Polytechnique Fédérale de Lausanne, CH-1015 Lausanne, Switzerland.

Electronic Supplementary Information (ESI) available: [see second file].
See DOI: 10.1039/b000000x/

1. B. Walker, C. Kim, and T.-Q. Nguyen, *Chem. Mater.*, 2011, **23**, 470–482.
2. Y. Sun, G. C. Welch, W. L. Leong, C. J. Takacs, G. C. Bazan, and A. J. Heeger, *Nat Mater*, 2011, **11**, 44–48.
3. Y. Liu, C.-C. Chen, Z. Hong, J. Gao, Y. M. Yang, H. Zhou, L. Dou, G. Li, and Y. Yang, *Sci Rep*, 2013, **3**, 3356.
4. S. Shoaee, S. Mehraeen, J. G. Labram, J.-L. Brédas, D. D. C. Bradley, V. Coropceanu, T. D. Anthopoulos, and J. R. Durrant, *J. Phys. Chem. Lett.*, 2014, **5**, 3669–3676.
5. A. Devižis, D. Hertel, K. Meerholz, V. Gulbinas, and J. E. Moser, *Organic Electronics*, 2014, **15**, 3729–3734.
6. J. Heier, J. Groenewold, S. Huber, F. Nüesch, and R. Hany, *Langmuir*, 2008, **24**, 7316–7322.
7. B. Fan, F. Araujo De Castro, J. Heier, R. Hany, and F. Nüesch, *Organic Electronics*, 2010, **11**, 583–588.
8. G. Wicht, S. Bücheler, M. Dietrich, T. Jäger, F. Nüesch, T. Offermans, J.-N. Tisserant, L. Wang, H. Zhang, and R. Hany, *Solar Energy Materials and Solar Cells*, 2013, **117**, 585–591.
9. S. Jenatsch, R. Hany, A. C. Véron, M. Neukom, S. Züfle, A. Borgschulte, B. Ruhstaller, and F. A. Nüesch, *J. Phys. Chem. C*, 2014, **118**, 17036–17045.
10. O. Malinkiewicz, T. Grancha, A. Molina-Ontoria, A. Soriano, H. Brine, and H. J. Bolink, *Adv. Energy Mater.*, 2012, **3**, 472–477.
11. A. Mishra, R. K. Behera, P. K. Behera, B. K. Mishra, and G. B. Behera, *Chem. Rev.*, 2000, **100**, 1973–2012.
12. M. Lloyd and J. Anthony, *Materials Today*, 2007, **10**, 34–41.
13. H. Benmansour, F. A. Castro, M. Nagel, J. Heier, R. Hany, and F. Nüesch, *CHIMIA*, 2007, **61**, 787–791.
14. A. C. Véron, H. Zhang, A. Linden, F. Nüesch, J. Heier, R. Hany, and T. Geiger, *Org. Lett.*, 2014, **16**, 1044–1047.
15. Z. Huang, D. Ji, S. Wang, A. Xia, F. Koberling, M. Patting, and R. Erdmann, *J. Phys. Chem. A*, 2006, **110**, 45–50.
16. K. Jia, Y. Wan, A. Xia, S. Li, F. Gong, and G. Yang, *J. Phys. Chem. A*, 2007, **111**, 1593–1597.
17. A. Chibisov and S. Shvedov, *Journal of Photochemistry and Photobiology*, 2001, **141**, 39–45.
18. L. Ferreira, A. Oliveira, and F. Wilkinson, *J Chem Soc*, 1996.
19. F. A. Castro, H. Benmansour, J.-E. Moser, C. F. O. Graeff, F. Nüesch, and R. Hany, *Phys. Chem. Chem. Phys.*, 2009, **11**, 8886–8894.
20. M. C. Etter, B. N. Holmes, R. B. Kress, and G. Filipoich, *Isr. J. Chem.*, 1984, **25**, 264–273.
21. G. B. Schuster, *Pure and applied chemistry*, 1990, **62**, 1565–1572.
22. B. Sauerwein and G. B. Schuster, *J. Phys. Chem.*, 1991, **95**, 1903–1906.
23. X. Yang, A. Zaitsev, B. Sauerwein, S. Murphy, and G. B. Schuster, *J. Am. Chem. Soc*, 1992, **114**, 793–794.
24. S. Chatterjee, P. Gottschalk, P. D. Davis, and G. B. Schuster, *J. Am. Chem. Soc*, 1988, **110**, 2326–2328.
25. S. Chatterjee, P. D. Davis, P. Gottschalk, M. E. Kurz, B. Sauerwein, X. Yang, and G. B. Schuster, *J. Am. Chem. Soc*, 1990, **112**, 6329–6338.
26. T. Konishi, Y. Sasaki, M. Fujitsuka, Y. Toba, H. Moriyama, and O. Ito, *J. Chem. Soc., Perkin Trans. 2*, 1999, 551–556.
27. J. D. Wilkey and G. B. Schuster, *J. Org. Chem.*, 1987, **52**, 2117–2122.

28. S. Chatterjee, P. D. Davis, P. Gottschalk, M. E. Kurz, B. Sauerwein, X. Yang, and G. B. Schuster, *J. Am. Chem. Soc*, 1990, **112**, 6329–6338.
29. J. Heier, C. Peng, A. C. Véron, R. Hany, T. Geiger, F. A. Nüesch, M. V. G. Vismara, and C. F. O. Graeff, eds. Z. H. Kafafi, P. A. Lane, and I. D. W. Samuel, SPIE, 2014, vol. 9184, p. 918408.
30. J. Guo, J. Guo, H. Ohkita, H. Ohkita, H. Benten, H. Benten, S. Ito, and S. Ito, *J. Am. Chem. Soc*, 2010, **132**, 6154–6164.
31. S. Cook, H. Ohkita, Y. Kim, and J. Benson-Smith, *Chemical Physics Letters*, 2007, **445**, 276–280.
32. D. Peckus, A. Devižis, R. Augulis, S. Graf, D. Hertel, K. Meerholz, and V. Gulbinas, *J. Phys. Chem. C*, 2013, **117**, 6039–6048.
33. A. Devižis, J. De Jonghe-Risse, R. Hany, F. Nüesch, S. Jenatsch, V. Gulbinas, and J.-E. Moser, 2015, submitted.

Kinetic competition between charge separation and intra-ion pair reductive quenching depends on acceptor concentration and phase intermixing morphology.